Phase-Modulation Based Dual-Function Radar-Communications

Aboulnasr Hassanien*, Moeness G. Amin*, Yimin D. Zhang†, and Fauzia Ahmad*

Abstract

We develop a novel phase-modulation based dual-function system with joint radar and communication platforms. A bank of transmit beamforming weight vectors is designed such that they form the same transmit power radiation patterns whereas the phase associated with each transmit beam towards the intended communication directions belongs to a certain phase-constellation. During each radar pulse, a binary sequence is mapped into one point of the constellation which, in turn, is embedded into the radar emission by selecting the transmit weight vectors associated with that constellation point. The communication receiver detects the phase of the received signal and uses it to decode the embedded binary sequence. The proposed technique allows information delivery to the intended communication receiver regardless of whether it is located in the sidelobe region or within the main radar beam. Three signaling strategies are proposed which can be used to achieve coherent communications, non-coherent communications, and non-coherent broadcasting, respectively. It is verified that the proposed method provides improved bit error performance as compared to previously reported sidelobe modulation based dual-functionality techniques.

Index Terms

Dual-function radar-communications, information embedding, phase-modulation, sidelobe control, bit error rate.

*A. Hassanien, M. G. Amin, and F. Ahmad are with the Center for Advanced Communications, College of Engineering, Villanova University, Villanova, PA 19085, USA (emails: {aboulnasr.hassanien; moeness.amin; fauzia.ahmad}@villanova.edu).

†Y. D. Zhang is with the Department of Electrical and Computer Engineering, College of Engineering, Temple University, Philadelphia, PA 19122, USA (email: ydzhang@temple.edu)

I. INTRODUCTION

Recently, the problem of radio frequency (RF) spectrum congestion has received considerable attention [1]–[8]. In particular, spectrum management and the coexistence of radar and communications have been the focus of intensive research [9]–[25]. Spectral congestion management via the waveform design and diversity paradigm has been reported in [26]–[30]. The coexistence of radar and communications can not only ease competition over bandwidth [1], [3], but can also enhance spectrum usage and efficiency in cognitive radio [17] and cognitive radar [18]. However, in order to enable sharing of spectrum resources and same bandwidth occupancy, effective approaches need to be devised for limiting cross-interference between the radar and communication system functions and properly utilizing the spatio-temporal degrees of freedom brought about by advances in waveform design and ubiquitous use of multi-sensor transmit/receive configurations.

Spectrum sharing and the use of common transmit platform between radar and communications require defining the primary and secondary system functions, as demanded by power allocations and preference in beam directivity. A method for embedding a covert message into the radar backscatter was addressed in [11]–[14]. The embedding of a communication signal into the radar emission was reported in [12], wherein the radar transmit waveform is selected from a bank of waveforms, each representing a communication symbol. Another method for information embedding uses time modulated arrays to introduce variations in the sidelobe level (SLL) towards the intended communication receiver [19]. During each radar pulse, the communication receiver detects the SLL and interprets the associated information symbol. Recently, a dual-function radar-communication (DFRC) system using waveform diversity in tandem with sidelobe control was introduced [21]. The essence of this DFRC system is to simultaneously transmit multiple orthogonal waveforms where each waveform is used in tandem with sidelobe shift keying to embed binary data. It was shown in [21] that the communication process is inherently secure against intercepts from directions other than the pre-assigned communication directions. It is noted that the methods in [19] and [21] enable communications within the sidelobe region only. The fact that the information embedding depends on the ability to modulate the signal amplitude transmitted towards the intended communication directions renders communication within the main radar beam infeasible, since the main beam is expected to remain unchanged during the entire processing interval.

In this paper, we propose a phase-modulation based method for embedding information into the radar emission. In order to deliver a message of N_b bits per radar pulse, a dictionary of $K = 2^{N_b}$ symbols is constructed. During each radar pulse, one phase symbol is embedded into the radar emission towards the intended communication direction. The communication receiver detects the embedded phase symbol and, subsequently, deciphers the corresponding binary sequence. Three phase-modulation based transmit signaling strategies are developed. The first strategy is suitable for coherent symbol embedding at the transmitter and symbol detection at the receiver, i.e., it requires phase synchronization between transmitter and receiver. The other two signaling strategies are noncoherent, one is suitable for directional communications, i.e., information embedding is directed towards a communication receiver located at a specific predetermined direction, and the other is applicable to broadcasting, i.e., the communication receiver can detect the embedded information regardless of the receiver directions.

For coherent communications, one radar waveform and a bank of K transmit beamforming weight vectors are required. Each phase symbol in the dictionary is associated with one transmit beamforming weight vector. The same radar waveform is used during all pulses, but the transmit beamforming weight vector changes from pulse to pulse depending on which phase symbol is embedded. Utilizing the principle of transmit radiation pattern invariance, all designed weight vectors are guaranteed to have the same transmit radiation pattern. The transmit radiation invariance property permits embedding of information towards communication receivers not only located within the sidelobe region but also within the main beam of the radar. For noncoherent communications, two orthogonal waveforms are used and the phase symbol is embedded as a phase rotation between two transmitted signal components, i.e., as the phase of the signal associated with the first transmit waveform relative to the phase associated with the second transmit waveform. Since both waveforms are emitted simultaneously and propagate through the same environments, the phase rotation is preserved. By estimating the phase rotations at the receiver, the embedded binary sequence can be obtained. It is worth noting that the use of two waveforms results in doubling the number of transmit beamforming weight vectors, i.e., during each radar pulse two weight vectors are used. This implies that a bank of $2K$ weight vectors required for the noncoherent case. The superiority of the proposed method over the recently developed methods in [19] and [21] is validated using simulation examples.

The remainder of paper is organized as follows. The signal model is described in Section

II. The proposed phase-modulation based information embedding method and the associated transmit signaling strategies are presented in Section III. Section IV provides a review of the two amplitude-modulation based methods for information embedding, previously reported in [19] and [21]. Supporting simulation results are presented in Section V and conclusions are drawn in Section VI.

II. SIGNAL MODEL

We consider a joint radar-communication platform equipped with M transmit antennas arranged as a uniform linear array. The radar receiver employs an array of N receive antennas with an arbitrary linear configuration. Without loss of generality, a single-element communication receiver is assumed to be located in direction θ_c, which is known to the transmitter. The joint radar-communications bandwidth is denoted as B and the total transmit power budget is P_t. Let $\psi_u(t)$ and $\psi_v(t)$ be two orthogonal radar waveforms, each occupying the same bandwidth B. In other words, the spectral contents of both waveforms overlap in the frequency domain. It is assumed that each waveform is normalized to have unit power, i.e. $\int_{T_p} |\psi_u(t)|^2 dt = \int_{T_p} |\psi_v(t)|^2 dt = 1$, where T_p is the radar pulse duration and t is the fast time index. It is further assumed that the orthogonality condition $\int_{T_p} \psi_u(t)\psi_v^*(t) dt = 0$ is satisfied, where $(\cdot)^*$ stands for the complex conjugate. The $M \times 1$ baseband signal vector at the input of the transmit antennas can be expressed as

$$\mathbf{s}(t) = \sqrt{P_u}\mathbf{u}^*\psi_u(t) + \sqrt{P_v}\mathbf{v}^*\psi_v(t), \tag{1}$$

where P_u and $\mathbf{u}$ denote the transmit power and the $M \times 1$ transmit beamforming weight vector associated with $\psi_u(t)$, respectively, and P_v and $\mathbf{v}$ denote the respective transmit power and the $M \times 1$ transmit beamforming weight vector associated with $\psi_v(t)$. In (1), the total transmit power satisfies $P_t = P_u + P_v$. The problem of transmit beamforming design considers the primary radar operation requirements, such as focusing the transmit power within the main beam region, keeping the sidelobe levels of the transmit radiation pattern below a certain predetermined threshold, and enforcing nulls towards jammers. The secondary communication function of the joint system is achieved by embedding information via controlling the phase of the signal radiated towards predetermined communication receivers with known directions.

Assume that L far-field targets of interest, located within the radar main beam, are observed in the background of strong clutter and interference. The $N \times 1$ baseband representation of the

signals at the output of the radar receive antenna array is given by

$$\mathbf{x}(t;\tau) = \sum_{\ell=1}^{L} \beta_\ell(\tau)\Big(\mathbf{a}^T(\theta_\ell)\mathbf{s}(t;\tau)\Big)\mathbf{b}(\theta_\ell) + \mathbf{x}_i(t;\tau) + \mathbf{z}(t;\tau), \qquad (2)$$

where τ is the slow-time index (i.e., pulse number) and $\beta_\ell(\tau)$ is the ℓth target reflection coefficient which obeys the Swerling II target model, i.e., it remains constant during the entire radar pulse but changes from pulse to pulse. In addition, $\mathbf{a}(\theta)$ and $\mathbf{b}(\theta)$ are the $M \times 1$ and the $N \times 1$ steering vectors of the transmit and receive arrays, respectively, $\mathbf{x}_i(t;\tau)$ is the $N \times 1$ vector summarizing the background interference plus clutter signal contributions, $\mathbf{z}(t;\tau)$ is the $N \times 1$ vector of additive white Gaussian noise with zero mean and covariance $\sigma_z^2 \mathbf{I}_N$, $(\cdot)^T$ stands for the transpose operation, and $\mathbf{I}_N$ denotes the $N \times N$ identity matrix. Post-processing of the received radar data can be performed with or without pulse compression [31], [32]. Pulse compression along with waveform diversity have proven to be a powerful tool in multiple-input multiple-output (MIMO) radar [32]–[39]. Therefore, in this paper, we adopt the use of pulse compression at the radar receiver. Matched-filtering the received data to the radar transmit waveforms yields the $2N \times 1$ vector of virtual received data

$$\mathbf{x}_{\mathrm{rad}}(\tau) = \mathrm{vec}\left(\int_{T_p} \mathbf{x}(t;\tau)\Psi^H(t)dt\right)$$

$$= \sum_{\ell=1}^{L} \beta_\ell(\tau)\tilde{\mathbf{a}}(\theta_\ell) \otimes \mathbf{b}(\theta_\ell) + \tilde{\mathbf{x}}_i(\tau) + \tilde{\mathbf{z}}(\tau), \qquad (3)$$

where $\mathrm{vec}(\cdot)$ denotes the vectorization of the columns of a matrix, $(\cdot)^H$ stands for the Hermitian operation, $\Psi(t) \triangleq [\psi_{\mathrm{u}}(t),\ \psi_{\mathrm{v}}(t)]^T$ is the vector of orthogonal waveforms, $\tilde{\mathbf{a}}(\theta_\ell) \triangleq [\sqrt{P_{\mathrm{u}}}\mathbf{u}^H\mathbf{a}(\theta_\ell),$ $\sqrt{P_{\mathrm{v}}}\mathbf{v}^H\mathbf{a}(\theta_\ell)]^T$ is the 2×1 transmit processing gain vector, $\tilde{\mathbf{x}}_i(\tau) \triangleq \mathrm{vec}\big(\int_{T_p} \mathbf{x}_i(t;\tau)\Psi^H(t)\big)$ is the $2N \times 1$ interference signal component at the output of the matched filter, and $\tilde{\mathbf{z}}(\tau)$ corresponds to the additive noise term with zero mean and covariance $\sigma_z^2 \mathbf{I}_{2N}$.

For the communication function of the proposed system, the waveform dictionary used at the transmitter is assumed to be known to the communication receiver. The baseband representation of the signal at the output of the communication receiver can be expressed as

$$y_{\mathrm{com}}(t;\tau) = \alpha_{\mathrm{ch}}(\tau)\mathbf{a}^T(\theta_c)\mathbf{s}(t;\tau) + n(t;\tau), \qquad (4)$$

where $\alpha_{\mathrm{ch}}(\tau)$ is the channel coefficient of the received signal which summarizes the propagation environment between the transmit array and the communication receiver during the τth pulse,

and $n(t; \tau)$ is the additive white Gaussian noise with zero mean and variance σ_c^2. Substituting (1) in (4) and matched-filtering the received communication signal to $\psi_{\mathrm{u}}(t)$ yields

$$
\begin{aligned}
y_{\mathrm{u}}(\tau) &= \sqrt{P_{\mathrm{u}}}\alpha_{\mathrm{ch}}(\tau)\Big(\mathbf{u}^H\mathbf{a}(\theta_c)\Big) + n_{\mathrm{u}}(\tau) \\
&= \sqrt{P_{\mathrm{u}}}\alpha_{\mathrm{ch}}(\tau)G_{\mathrm{u}}e^{j\phi_{\mathrm{u}}} + n_{\mathrm{u}}(\tau),
\end{aligned}
\tag{5}
$$

where $G_{\mathrm{u}} \triangleq |\mathbf{u}^H\mathbf{a}(\theta_c)|$ and $\phi_{\mathrm{u}} \triangleq \mathrm{angle}\big(\mathbf{u}^H\mathbf{a}(\theta_c)\big)$ are the magnitude and phase of the transmit beamforming complex gain towards the communication direction associated with ψ_{u}, respectively, $n_{\mathrm{u}}(\tau)$ is white Gaussian noise term at the output of the matched filter with zero mean and variance σ_c^2, and $|\cdot|$ and $\mathrm{angle}(\cdot)$ stand for the magnitude and angle of a complex number, respectively. Similarly, matched-filtering $y_{\mathrm{com}}(t; \tau)$ to the waveform $\psi_{\mathrm{v}}(t)$ yields

$$
\begin{aligned}
y_{\mathrm{v}}(\tau) &= \sqrt{P_{\mathrm{v}}}\alpha_{\mathrm{ch}}(\tau)\Big(\mathbf{v}^H\mathbf{a}(\theta_c)\Big) + n_{\mathrm{v}}(\tau) \\
&= \sqrt{P_{\mathrm{v}}}\alpha_{\mathrm{ch}}(\tau)G_{\mathrm{v}}e^{j\phi_{\mathrm{v}}} + n_{\mathrm{v}}(\tau),
\end{aligned}
\tag{6}
$$

where $G_{\mathrm{v}} \triangleq |\mathbf{v}^H\mathbf{a}(\theta_c)|$ and $\phi_{\mathrm{v}} \triangleq \mathrm{angle}\big(\mathbf{v}^H\mathbf{a}(\theta_c)\big)$ are the magnitude and phase of the transmit beamforming gain towards the communication direction associated with ψ_{v}, respectively, and $n_{\mathrm{v}}(\tau)$ is white Gaussian noise term at the output of the matched filter with zero-mean and variance σ_c^2.

During each radar pulse, phase-modulation based communications can be achieved by selecting the phases ϕ_{u} and ϕ_{v} from a predefined phase constellation. The embedded information can be detected at the communication receiver by estimating the embedded phases. Phase estimation requires phase synchronization between the joint transmitting platform and the communication receiver. In this case, the communication process is coherent.

It is worth noting that, if $\mathbf{u}$ and $\mathbf{v}$ are appropriately designed such that the condition $\sqrt{P_u}G_{\mathrm{u}} = \sqrt{P_v}G_{\mathrm{v}}$ (i.e. $\sqrt{P_u}|\mathbf{u}^H\mathbf{a}(\theta_c)| = \sqrt{P_u}|\mathbf{v}^H\mathbf{a}(\theta_c)|$) is satisfied, then $y_{\mathrm{u}}(\tau)$ and $y_{\mathrm{v}}(\tau)$ are guaranteed to enjoy the so-called rotational invariance property. This property implies that the noise-free version of $y_{\mathrm{u}}(\tau)$ equals the noise-free version of $y_{\mathrm{v}}(\tau)$ up to some phase rotation $\breve{\phi}$. This phase rotation can be expressed as

$$
\breve{\phi} = \mathrm{angle}\left(\frac{\mathbf{u}^H\mathbf{a}(\theta_c)}{\mathbf{v}^H\mathbf{a}(\theta_c)}\right) = \phi_{\mathrm{u}} - \phi_{\mathrm{v}}.
\tag{7}
$$

Information embedding can be achieved by controlling the value of the phase rotation at the transmit side, i.e., by selecting the phase rotation from a predefined constellation. It is worth

noting that both waveforms are radiated simultaneously and propagate through the same environment. Therefore, any phase synchronization error that occurs due to, for example, propagation distortion, yields the same phase error in both $y_{\mathrm{u}}(\tau)$ and $y_{\mathrm{v}}(\tau)$. This results in a common phase term in the numerator and denominator of (7) which has no effect on the phase rotation. Since measuring the phase associated with one waveform with respect to the phase associated with the other waveform cancels out any common phase term, the common initial phase at the transmit array and/or the common phase error terms have no effect on the estimation of the phase rotation at the receiver. Therefore, employing a phase decoder at the communication receiver does not require phase synchronization and, therefore, the communication process in this case is non-coherent.

In the remainder of the paper, we present several transmit signaling strategies and show how to appropriately design the transmit beamforming weight vectors in order to achieve a desired phase constellation.

III. PHASE-MODULATION BASED INFORMATION EMBEDDING

In this section, we introduce phase-modulation based method for embedding information into the radar emission. More specifically, three phase-modulation based transmit signaling strategies are proposed. The associated transmit beamforming design and phase-constellation formation are also presented.

A. Transmit Beamforming Design

We start with an $M \times 1$ principal transmit beamforming weight vector $\mathbf{w}$, which satisfies a certain desired transmit power radiation pattern. The main function of $\mathbf{w}$ is to concentrate the transmit power within a certain desired spatial sector $\boldsymbol{\Theta} = [\theta_{\mathtt{min}}, \ \theta_{\mathtt{max}}]$ while minimizing the power radiated in the out-of-sector region $\bar{\boldsymbol{\Theta}}$. Extension to multiple sector cases is straightforward. Sophisticated methods for designing a single transmit beamforming weight vector that achieves a desired pattern with ripple and transition band properties have been reported in the literature (see [38], [37] and references therein). One way of designing $\mathbf{w}$ is by solving the following optimization problem [39]

$$\min_{\mathbf{w}} \max_{i} \left| \mathbf{w}^H \mathbf{a}(\theta_i) - e^{j\mu(\theta_i)} \right|, \quad \theta_i \in \boldsymbol{\Theta}, \ i = 1, \dots, I$$

$$\text{subject to } \left| \mathbf{w}^H \mathbf{a}(\theta_p) \right| \leq \varepsilon, \quad \theta_p \in \bar{\boldsymbol{\Theta}}, \ p = 1, \dots, P, \tag{8}$$

where θ_i, $i = 1, \ldots, I$ and θ_p, $p = 1, \ldots, P$ are continuums of angles chosen respectively, uniformly or non-uniformly from Θ and $\bar{\Theta}$, to approximate these two sectors, $\mu(\theta)$ is an arbitrary phase profile which is assumed to be continuous within the desired sector Θ, and ε is a user-specified positive number to control sidelobe levels. The optimization problem (8) is convex and can be efficiently solved using the interior point methods [40].

The $M \times 1$ principal weight vector can be used to generate a population of 2^{M-1} weight vectors of the same dimensionality, all having the same transmit power radiation pattern as that of $\mathbf{w}$ [41], [42]. The aforementioned population, denoted as $\mathbf{W} = \{\mathbf{w}_1, \ldots, \mathbf{w}_{2^{M-1}}\}$, can be obtained by viewing the principal weight vector as a polynomial of order $M - 1$ with the $M - 1$ roots denoted as r_i, $i = 1, \ldots, M - 1$. Note that reflecting each root against the unit circle does not change the magnitude of the beampattern. At most 2^{M-1} different polynomials of the same order can be constructed, depending on the employed $M - 1$ combinations of the roots r_i (or $1/r_i^*$), $i = 1, \cdots, M - 1$, for polynomial construction [41]. It is worth noting that $2^M - 1$ unique polynomials can be obtained as long as the zeros do not lie on the unit circle.

B. Coherent Phase-Modulation Based Communications

For coherent communication embedding, a single radar waveform can be used. This enables information embedding into the radar emission for the case of a single-input multiple-output (SIMO) radar operation. In this case, $P_{\mathrm{u}} = P_{\mathrm{t}}$ and $P_{\mathrm{v}} = 0$, and the transmit signal model in (1) simplifies to

$$\mathbf{s}(t) = \sqrt{P_{\mathrm{t}}}\mathbf{u}^*\psi_{\mathrm{u}}(t). \tag{9}$$

During each radar pulse, an N_b bit information message composed of 1's and 0's, denoted as the binary sequence b_n, $n = 1, \ldots, N_b$ is mapped into a dictionary of $K = 2^{N_b}$ phase symbols denoted as $\mathbb{D}_{\mathrm{PM}} = \{\Omega_1, \ldots, \Omega_K\}$, where Ω_k denotes the kth phase symbol. Ideally, the constellation Ω_k can be chosen to be uniformly distributed on the unit circle. In order to embed N_b-bit message in the radar emission, the corresponding phase symbol should be embedded in the transmitted signal. We build a transmit beamforming weight dictionary consisting of K vectors denoted as $\mathbb{U} = \{\mathbf{u}_1, \ldots, \mathbf{u}_K\}$ where the kth weight vector is associated with the kth phase symbol Ω_k. The kth weight vector can be chosen based on the following criterion

$$\min_{\mathbf{u}_k} \left|\Omega_k - \mathrm{angle}(\mathbf{u}_k^H \mathbf{a}(\theta_c))\right| \quad \text{s.t.} \quad \mathbf{u}_k \in \mathbf{W}. \tag{10}$$

To ensure unique one-to-one relationship between $\mathbb{D}_{\mathrm{PM}}$ and $\mathbb{U}$, we enforce the condition $\mathbf{u}_k \neq \mathbf{u}_{k'}$, $k \neq k'$ while solving (10).

Depending on the actual bit sequence to be embedded during a certain radar pulse and the associated phase symbol, $\mathbf{u}$ in (9) should be chosen from $\{\mathbf{u}_1, \ldots, \mathbf{u}_K\}$. Assume that Ω_k is embedded during a certain pulse, then the received communication signal at the output of the matched filter (5) simplifies to

$$y_{\mathrm{u}}(\tau) = \sqrt{P_{\mathrm{t}}}\alpha_{\mathrm{ch}}(\tau)G_{\mathrm{u}}e^{j\phi_{\mathrm{u}}} + n_{\mathrm{u}}(\tau), \tag{11}$$

and the embedded phase can be estimated at the communication receiver as

$$\hat{\phi}(\tau) = \mathrm{angle}(y_{\mathrm{u}}(\tau)). \tag{12}$$

The actual embedded binary message can be decoded by comparing the phase estimate to the K dimensional phase dictionary $\phi_1, \ldots, \phi_K$, where

$$\phi_k = \mathrm{angle}\left(\mathbf{u}_k^H \mathbf{a}(\theta_c)\right). \tag{13}$$

It is worth noting that the accurate detection of the embedded message requires perfect phase synchronization between the joint radar-communication transmit platform and the communication receiver. Any synchronization mismatch will result in performance degradation. In the next subsection, we introduce a non-coherent information embedding strategy.

C. Non-Coherent Phase-Modulation Based Communications

To avoid degradation in the performance of the communication system due to transmit-receive phase synchronization errors and/or inaccurate channel coefficient estimation, we propose a non-coherent phase-modulation based communication embedding into the radar emission. The information message is embedded in the phase difference between the radar signal associated with the two waveforms. We build a transmit beamforming weight dictionary using K pairs of weight vectors denoted as $\{\mathbf{u}_1, \mathbf{v}_1\}, \ldots, \{\mathbf{u}_K, \mathbf{v}_K\}$ which can be chosen from the population $\mathbf{W}$. The phase difference associated with the kth pair is given by

$$\varphi_k = \mathrm{angle}\left(\frac{\mathbf{u}_k^H \mathbf{a}(\theta_c)}{\mathbf{v}_k^H \mathbf{a}(\theta_c)}\right). \tag{14}$$

The beamforming weight vector pair, which yields the closest phase-rotation φ_k to the corresponding desired phase symbol Ω_k, can be selected from the population $\mathbf{W}$ as follows:

$$\min_{\mathbf{u}_k, \mathbf{v}_k} \left| \text{angle}(\mathbf{u}_k^H \mathbf{a}(\theta_c)) - \text{angle}(\mathbf{v}_k^H \mathbf{a}(\theta_c)) - \Omega_k \right| \quad \text{s.t.} \quad \{\mathbf{u}_k, \mathbf{v}_k\} \in \mathbf{W}. \tag{15}$$

Only one of the K phase-rotational symbols is embedded during each radar pulse to deliver the N_b bits of information. Assuming that the total transmit power is split equally between the two radar waveforms being used, the transmit signal model (1) is rewritten as

$$\mathbf{s}(t) = \sqrt{\frac{P_t}{2}} \Big(\mathbf{u}^* \psi_u(t) + \mathbf{v}^* \psi_v(t) \Big). \tag{16}$$

With the kth phase-rotation symbol embedded on transmit, the respective out signals of the two matched filters at the communication receiver are given as

$$y_u(\tau) = \sqrt{\frac{P_t}{2}} \alpha_{ch}(\tau) \Big(\mathbf{u}_k^H \mathbf{a}(\theta_c) \Big) + n_u(\tau), \tag{17}$$

and

$$y_v(\tau) = \sqrt{\frac{P_t}{2}} \alpha_{ch}(\tau) \Big(\mathbf{v}_k^H \mathbf{a}(\theta_c) \Big) + n_v(\tau). \tag{18}$$

As a result, the phase-rotation embedded in the received signal can be estimated as

$$\hat{\varphi}(\tau) = \text{angle}\Big(\frac{y_u(\tau)}{y_v(\tau)} \Big). \tag{19}$$

The actual sequence of embedded bits can be determined by comparing $\hat{\varphi}(\tau)$ obtained from (19) to the phase-rotation dictionary (14) and mapping it to the corresponding binary sequence.

It is worth noting that both coherent and non-coherent information embedding strategies are angle dependent, i.e., they allow receivers located at the intended communication direction to detect the embedded message. The ability to detect the embedded information from directions other than the intended communication direction is limited especially for large constellation size.

D. Phase-Modulation Based Broadcast

The information embedding strategies introduced in Subsections III-B and III-C are angle dependent, i.e., the used phase symbols are functions of the communication direction. This enables secure communications towards a finite number of communication directions. However, there are practical situations where the direction of the communication receiver is either unknown or rapidly changing. Another applicable situation is the broadcast systems where multiple intended

receivers are distributed over different directions. A meaningful way to handle such cases is to embed information in broadcast mode. This can be achieved by selecting $\mathbf{v}_k$ as a rotated version of $\mathbf{u}_k$, that is,

$$\mathbf{v}_k = \mathbf{u}_k e^{-j\Omega_k}, \qquad k = 1, \ldots, K. \tag{20}$$

Note that for any arbitrary direction θ, the phase difference between the signals associated with the kth broadcast vector pair $\{\mathbf{u}_k, \mathbf{v}_k\}$ is given by

$$\varphi_k = \text{angle}\left(\frac{\mathbf{u}_k^H \mathbf{a}(\theta)}{\mathbf{v}_k^H \mathbf{a}(\theta)} \right)$$
$$= \text{angle}\left(\frac{\mathbf{u}_k^H \mathbf{a}(\theta)}{\mathbf{u}_k^H \mathbf{a}(\theta)} \cdot e^{j\Omega_k} \right) = \Omega_k. \tag{21}$$

This implies that the phase difference between the two signals is constant regardless of the direction at which the communication receiver is located, i.e., the broadcast message can be detected from any arbitrary direction via estimating the phase-difference. However, as the transmit processing gain $G(\theta) = |\mathbf{u}_k^H \mathbf{a}(\theta)| = |\mathbf{v}_k^H \mathbf{a}(\theta)|$ is angle dependent, the detection performance depends on whether the communication receiver is located within the radar mainlobe or the sidelobe region. In particular, receivers located within the main radar beam will be able to decode the embedded signal with much higher quality as compared to receivers located in the sidelobe region.

It is worth noting that broadcast signaling strategy based on (20) enables embedding the exact desired phase symbols Ω_k, $k = 1, \ldots, K$, i.e., the actual phase-rotation dictionary used (21) is the exact desired phase dictionary Ω_k. On the other hand, for the non-coherent directional phase-modulation based communications discussed in Sec. III-C, the actual phase-rotation dictionary obtained by solving (15) is guaranteed to be as close as possible to the desired phase symbols Ω_k, $k = 1, \ldots, K$ but not necessarily identical. However, for large values of M, the number 2^{M-1} of weight vectors to choose from while solving (15) becomes very large, thus making it easier to achieve the exact desired phase dictionary.

Substituting (20) in (16) and assuming that the kth symbol is embedded, the transmit signal simplifies to

$$\mathbf{s}(t) = \sqrt{\frac{P_t}{2}} \left(\psi_u(t) + e^{-j\Omega_k} \psi_v(t) \right) \mathbf{u}_k^*$$
$$= \sqrt{\frac{P_t}{2}} \tilde{\psi}(t) \mathbf{u}_k^*, \tag{22}$$

where $\tilde{\psi}(t) \triangleq \psi_{\mathrm{u}}(t) + e^{-j\Omega_k}\psi_{\mathrm{v}}(t)$. This means that the radar transmitter operates in a SIMO mode, i.e., at the radar receiver, pulse compression is achieved via matched filtering the radar received signal to $\tilde{\psi}(t)$.

The phase-rotation embedded in the received signal can be estimated using (19). The actual embedded sequence can be determined by comparing the estimated phase to the phase-rotation dictionary Ω_k, $k = 1, \ldots, K$, and mapping it to the corresponding binary sequence.

IV. SIDELOBE CONTROL BASED INFORMATION EMBEDDING

For the sake of comparison, in this section, we briefly review the two DFRC methods reported in [19] and [21]. The essence of these two methods is to embed information into the radar emission via amplitude modulation of the SLL towards the intended communication direction. Both methods enable information delivery to a communications receiver located within the sidelobe region of the radar. The method in [19] utilizes a single radar waveform and requires $K = 2^{N_b}$ distinct SLLs in order to embed N_b bits of information during each radar pulse. Achieving this number of distinct SLLs requires the design of K transmit beamforming weight vectors. Some practical considerations should be taken into account while designing the K weight vectors. From the radar operation view point, one key requirement is to maintain a constant transmit power radiation pattern within the main beam of the radar during the entire dwell time, i.e., during the coherent processing interval.

Assuming that the radar operation takes place in a wider spatial sector $\boldsymbol{\Theta} = [\theta_{\min} \ \theta_{\max}]$, one way to design the transmit beamforming weight vectors is to minimize the difference between the desired and actual transmit power radiation patterns under the constraints that the sidelobes be bounded by certain pre-defined levels. This can be formulated as the following optimization problem

$$\min_{\mathbf{u}_k} \max_{\theta_i} \left| e^{j\varphi(\theta_i)} - \mathbf{u}_k^H \mathbf{a}(\theta_i) \right|, \ \theta_i \in \boldsymbol{\Theta}, \ i = 1, \ldots, I \tag{23}$$

$$\text{subject to } \left| \mathbf{u}_k^H \mathbf{a}(\theta_p) \right| \leq \varepsilon, \quad \theta_p \in \bar{\boldsymbol{\Theta}}, \ p = 1, \ldots, P, \tag{24}$$

$$\mathbf{u}_k^H \mathbf{a}(\theta_c) = \Delta_k, \tag{25}$$

where Δ_k is a user-controlled positive number which corresponds to the kth SLL towards the communication direction θ_c. The value of Δ_k can be chosen from two or multiple SLLs depending on whether one or more bits are to be transmitted during each radar pulsedepending on whether

one or more bits are to be transmitted during each radar pulse. In (23)–(25), the objective function fits the actual transmit pattern associated with each transmit beam which is mandated by the radar operation. The set of constraints in (24) is used to upper-bound the transmit power leakage within the sidelobe areas, which is also mandated by the radar operation. Note that the upper bound determined by the parameter ε is the same for all transmit beams. The set of constraints in (25) is associated with the secondary function of the system, which is to embed information by enforcing different SLLs towards the communication directions. It is worth noting that the parameter Δ_k, which determines the SLL, is different for each transmit beam. Since ε is the highest sidelobe level as mandated by the main radar operation of the system, the condition $\Delta_k \leq \varepsilon, \; k = 1, \ldots, K$ should be satisfied. However, a tradeoff between the primary radar and the secondary communication operations can be achieved by allowing the SLLs towards the communication directions to be higher than the rest of the sidelobe region. This means that more transmit power is assigned to the communication operation at the price of a decreased transmit gain within the main radar beam. In this case, the set of constraints in (24) should cover the sidelobe region excluding the communication directions.

The optimization problem (23)–(25) is convex and can be solved in a computationally efficient manner [40]. However, the parameter ε should be carefully chosen to warrant a feasible solution. Note that the transmit beamforming weight vector obtained by solving (23)–(25) is normalized with a unit magnitude within the main radar beam. The actual transmit weight vector is scaled up to the desired transmit gain as long as the total transmit power budget does not exceed the maximum allowed power of the actual system. Further note that scaling up the transmit weight vector results in magnifying the transmit power distribution at all angles equally, i.e., the relative SLLs with respect to the mainlobe remain unchanged.

A. Information-Embedding Via Sidelobe Control

Assume that the kth symbol is embedded in the τth pulse. Then, the method in [19] models the signal transmitted during this pulse as

$$\mathbf{s}(t; \tau) = \sqrt{P_\mathrm{t}} \mathbf{u}_k \psi(t), \tag{26}$$

The signal at the output of the matched-filter at the communication receiver in this case is given as

$$
\begin{aligned}
y_{\mathrm{c}}(\tau) &= \sqrt{P_{\mathrm{t}}}\alpha_{\mathrm{ch}}(\tau)\Big(\mathbf{u}_k^H \mathbf{a}(\theta_c)\Big) + n(\tau) \\
&= \sqrt{P_{\mathrm{t}}}\alpha_{\mathrm{ch}}(\tau)\Delta_k + n(\tau).
\end{aligned}
\tag{27}
$$

Measuring the signal strength at the receiver as $\eta_{\mathrm{SLL}}(\tau) = |y_{\mathrm{c}}(\tau)|$, the transmitted symbol can be detected by comparing η_{SLL} to a set of $K-1$ thresholds $T_k,\ k = 1,\ldots,K-1$, that divide the K SLLs in an appropriate manner. Then, the detected symbol can be converted to the corresponding bit sequence.

B. Information-Embedding Via Sidelobe Control and Waveform Diversity

This subsection briefly reviews a method for information-embedding using waveform diversity in tandem with sidelobe control [21]. This method uses only two transmit beamforming weight vectors denoted as $\mathbf{u}_{\mathrm{H}}$ and $\mathbf{u}_{\mathrm{L}}$. Both $\mathbf{u}_{\mathrm{H}}$ and $\mathbf{u}_{\mathrm{L}}$ are assumed to have the same transmit power radiation pattern except in the spatial directions of the communication receivers where the SLL associated with $\mathbf{u}_{\mathrm{H}}$ is assumed to be higher than the SLL associated with $\mathbf{u}_{\mathrm{L}}$. The optimization problem (23)–(25) can be used for designing the aforementioned two weight vectors by choosing $\Delta_k = \Delta_{\mathrm{H}}$ while designing $\mathbf{u}_{\mathrm{H}}$ and $\Delta_k = \Delta_{\mathrm{L}}$ for designing $\mathbf{u}_{\mathrm{L}}$, where $\Delta_{\mathrm{H}} > \Delta_{\mathrm{L}}$. Therefore, the constraint in (25) should be restated as $\mathbf{u}_{\mathrm{H}}^H \mathbf{a}(\theta_c) = \Delta_{\mathrm{H}}$ and $\mathbf{u}_{\mathrm{L}}^H \mathbf{a}(\theta_c) = \Delta_{\mathrm{L}}$ while designing $\mathbf{u}_{\mathrm{H}}$ and $\mathbf{u}_{\mathrm{L}}$, respectively.

In addition to $\mathbf{u}_{\mathrm{H}}$ and $\mathbf{u}_{\mathrm{L}}$, the method requires that the number of orthogonal waveforms equals to the number of transmit bits per radar pulse, i.e., N_b waveforms are transmitted simultaneously. During each radar pulse, every transmitted orthogonal waveform is used to deliver one information bit to the communication receiver. The nth orthogonal waveform $\psi_n(t),\ n = 1,\ldots,N_b$, is radiated either via $\mathbf{u}_{\mathrm{H}}$ for $b_n(\tau) = 0$ or $\mathbf{u}_{\mathrm{L}}$ when $b_n(\tau) = 1$. In this case, the baseband transmit signals can be written as

$$
\mathbf{s}(t;\tau) = \sqrt{\frac{P_{\mathrm{t}}}{N_b}} \sum_{n=1}^{N_b} \Big(b_n(\tau)\mathbf{u}_{\mathrm{L}}^* + (1 - b_n(\tau))\mathbf{u}_{\mathrm{H}}^* \Big)\psi_n(t).
\tag{28}
$$

Note that that the total transmit power P_{t} is divided equally among the N_b waveforms.

At the communication receiver, the baseband representation of the received signal is given by

$$y_c(t;\tau) = \sqrt{\frac{P_t}{N_b}}\alpha_{ch}(\tau)\sum_{n=1}^{N_b}\Big(b_n(\tau)\mathbf{u}_L^H\mathbf{a}(\theta_c)$$

$$+\big(1-b_n(\tau)\big)\mathbf{u}_H^H\mathbf{a}(\theta_c)\Big)\psi_n(t) + \mathbf{n}_c(t;\tau)$$

$$= \sqrt{\frac{P_t}{N_b}}\alpha_{ch}(\tau)\sum_{n=1}^{N_b}\Big(b_n(\tau)\Delta_L + (1-b_n(\tau))\Delta_H\Big)\psi_n(t) + n_c(t;\tau). \tag{29}$$

Matched-filtering the received data in (29) to each of the transmitted orthogonal waveforms yields the data sets $y_n(\tau),\ n=1,\ldots,N_b$, expressed as

$$y_n(\tau) = \begin{cases} \sqrt{\frac{P_t}{N_b}}\alpha_{ch}(\tau)\Delta_H + n_n(\tau), & b_n(\tau)=0, \\ \\ \sqrt{\frac{P_t}{N_b}}\alpha_{ch}(\tau)\Delta_L + n_n(\tau), & b_n(\tau)=1, \end{cases} \tag{30}$$

where $n_n(\tau)$ is the additive noise at the output of the nth matched-filter with the same statistics as that of $n_c(t;\tau)$.

The transmitted bits can be detected by performing the following ratio test

$$\hat{b}_n(\tau) = \begin{cases} 0, & \text{if } |y_n(\tau)| \geq T_0, \\ \\ 1, & \text{if } |y_n(\tau)| < T_0, \end{cases} \tag{31}$$

where T_0 is a threshold. Note that the embedding and detection of each bit are independently performed from other bits due to the independence between the employed radar waveforms.

A few comments are in order with regards to the data rates that can be achieved using the SLL amplitude-modulated based DFRC methods. It is worth noting that most modern pulsed radar systems support pulse repetition frequencies in the kHz range [43]–[45] and, therefore, by embedding few bits per pulse, an overall data rate in the range of kbits per sec can be achieved. When the number of transmit array elements is large, higher values of N_b can be used leading to higher data rates. In addition to the waveform diversity, incorporating other types of diversity, e.g., polarization, offers the potential for achieving even higher data rates.

V. SIMULATION RESULTS

For all simulation examples presented in this section, we consider a uniform linear transmit array consisting of $M=10$ antennas spaced half wavelength apart, and assume that $N_b=2$ bits are embedded during each radar pulse.

Example 1: Transmit Power Radiation Pattern and Phase Constellation Design

We investigate the possibility of realizing multiple pairs of transmit beamforming weight vectors which have a certain desired transmit power distribution pattern as well as a desired phase-rotation dictionary. We assume that the main radar operation takes place within the sector $\Theta = [-10° \ 10°]$. A single communication direction of $\theta_c = -50°$ is assumed. We design the principal transmit beamforming weight vector by solving the following optimization problem

$$\min_{\mathbf{w}} \max_{i} \ \left| \mathbf{w}^H \mathbf{a}(\theta_i) - e^{j\pi\sin(\theta_i)} \right|, \quad \theta_i \in \Theta, \ i = 1, \dots, I$$

$$\text{subject to} \ \left| \mathbf{w}^H \mathbf{a}(\theta_p) \right| \leq \varepsilon, \quad \theta_p \in \bar{\Theta}, \ p = 1, \dots, P, \tag{32}$$

$$\mathbf{w}^H \mathbf{a}(\theta_c) = \varepsilon, \tag{33}$$

It is assumed that the radar operation requires the power level emitted in the sidelobe areas to be at least 20 dB lower than the mainlobe and, therefore, $\varepsilon = 0.1$ is chosen. Note that the constraint (33) determines the SLL towards the communication direction which is chosen to be equal to the highest allowable level, i.e., $\varepsilon_c = 0.1$ is used. The values $I = 200$ and $P = 140$ are used to approximate the desired sector and the out-of-sector regions, respectively. Fig. 1 shows the transmit power distribution versus the spatial angle for the principal transmit beamforming weight vector. It is clear from the figure that the SLLs are 20 dB below the mainlobe level and that the SLL towards the communication direction attain the maximum allowable value.

To embed $N_b = 2$ bits, a phase constellation of 4 symbols is assumed, that is $\Omega_k \in \{-\frac{\pi}{2}, 0, \frac{\pi}{2}, \pi\}$. The principal weight vector obtained by solving (32)–(33) is used to generate a population of $2^{M-1} = 512$ weight vectors which have exactly the same transmit power radiation patterns. For the proposed coherent phase-modulation based method, 4 weight vectors are chosen from the 512 population by solving (10). To implement the proposed non-coherent phase-modulation based method, the weight population is used to build 256 pairs of vectors and the phase rotations associated with the communication direction $\theta_c = -50°$ for all available pairs are plotted in Fig. 2. The figure shows that the available phase-rotations cover the entire phase domain between $0°$ and $360°$. This enables choosing a suitable phase-rotation dictionary of $K = 4$ pairs by solving (15). One realization for this case is indicated by the red circles in Fig. 2. It can be observed from the figure that the $K = 4$ phase-rotation dictionary is almost uniformly distributed on the unit circle, leading to a better probability of detection at the receiver. For the proposed

phase-modulation based broadcast method, the 4 pairs are chosen as $\mathbf{u}_k = \mathbf{w}$, $k = 1, \ldots, 4$ and $\mathbf{v}_k = \mathbf{w}e^{-j\Omega_k}$, $k = 1, \ldots, 4$.

Example 2: BER Performance Within the Sidelobe Region

In this example, we investigate the performance of the proposed phase-modulation based methods in terms of the bit error rate (BER)and compare with that of the sidelobe control based techniques summarized in Sec. IV. For the proposed methods, we use the same parameters and weight vectors as in the previous example. The phase-rotation dictionary of dimension $K = 4$, which corresponds to the red circles in Fig. 2, is used. Note that the method described in [19] does not employ waveform diversity. Instead, it employs a single waveform in tandem with 2^{N_b} SSLs towards the communication direction to deliver N_b bits of information. To deliver $N_b = 2$ bits, the method in [19] uses four transmit beamformers with four distinct SSLs towards the communication direction. These four weight vectors can be designed by solving the optimization problem (23)–(25) four times for $\Delta_1 = 0.1$, $\Delta_2 = \sqrt{0.0033}$, $\Delta_3 = \sqrt{0.0066}$ and $\Delta_4 = 0.01$, respectively. For the method of [21], two transmit weight vectors are used along with two orthogonal waveforms. In particular, the two weight vectors associated with $\Delta_1 = 0.1$ and $\Delta_4 = 0.01$ are used to implement the method of [21].

To compute the BER, a long sequence of 2×10^7 bits is randomly generated. During each radar pulse, two bits are embedded, i.e., the process of embedding/detecting two bits at a time is independently repeated 10^7 times. The propagation coefficient α_c is modeled as a random variable with a constant unit magnitude and uniformly distributed random phase. Fig. 3 depicts the BERs for the five methods tested versus the signal-to-noise ratio (SNR). It is clear that the three proposed phase-modulation based methods achieve superior BER performances as compared to the sidelobe control based methods. It can be observed from the figure that the proposed coherent phase-modulation based method achieves better BER performance as compared to the proposed non-coherent phase-modulation based methods. This is attributed to the fact that the coherent method assigns the total transmit power to a single waveform at the price that precise phase synchronization should be utilized. On the other hand, the two proposed non-coherent methods divide the transmit power between two waveforms while requiring no phase synchronization.

Example 3: BER Performance Within Main beam of the Transmit Power Pattern

We test the ability to communicate within the main radar beam. We assume that a communication receiver is located within the main beam at direction $\theta_c = 7.5°$. All setup parameters are chosen to be the same as in Example 2 except that the weight vectors needed to implement the coherent method and the four weight vector pairs needed to implement the non-coherent method are selected from the 512 weight vector population by solving (10) and (15), respectively, using $\theta_c = 7.5°$. For the non-coherent broadcast method, the same pairs of weight vectors from Example 2 are used. Fig. 4 shows the BER versus SNR for all methods tested. It is evident from the figure that the sidelobe control based methods totally fail to decode the embedded messages simply because they are designed to communicate within sidelobe region only. The BER curves for the three proposed phase-modulation based methods mirror the curves for the same methods in Fig. 4 except for a 20 dB shift on the SNR axis. This is due to the fact that the transmit processing gain within the main radar beam is 20 dB higher than the SLL. As a result, communications within the main radar beam is achieved with a much higher accuracy.

Example 4: BER Versus Angle

In this example, we test the possibility that an eavesdropper is able to receive/decode the embedded information from directions other than the intended communication direction. The simulation parameters are the same as in Example 3. In particular, we assume that the intended communication receiver is located at $\theta_c = 7.5°$. We assume that the eavesdropper has perfect knowledge of both the employed waveforms and the information embedding strategy. Fig. 5 depicts the BER versus the spatial angle with the SNR fixed to 0 dB for all methods. As expected, the sidelobe control based methods fail to decode any message from any direction including the true communication direction. Further, the proposed non-coherent phase-modulation based method with directional capabilities achieves its lowest BER at direction $\theta = \theta_c$. As the actual direction of the communication receiver deviated from the intended communication direction, the BER deteriorates. Moreover, the BER performance of the proposed non-coherent phase-modulation based broadcast method is flat regardless of the direction of the communication receiver. Finally, the BER performance of the proposed coherent phase-modulation based method is the lowest as compared to all other methods at $\theta = \theta_c$. However, it is also noted from Fig. 5 that the information embedded using the coherent phase-modulation based method can be

detected with high accuracy from some random directions other than the intended communication direction. This is because, for a phase dictionary of size $K = 4$, the coherent phase constellation obtained using (13) represents a linear system of four equations while the number of degrees-of-freedom equals M. Therefore, it is possible for the system of equations in (13) to have other solutions for $\theta \neq \theta_c$. Once the size of the constellations becomes larger than M the solution to (13) becomes unique.

We repeat the same example for the case when the intended communication receiver is located within the sidelobe region. The simulation parameters are the same as in Example 2 except that $N_b = 3$ bits per pulse, i.e., the constellation size is $K = 8$. Fig. 6 depicts the BER versus the spatial angle within that portion of the sidelobe region where the intended communication receiver is located. The SNR is fixed at 20 dB for all methods. The figure shows that for all methods tested, the embedded message cannot be detected reliably from directions other than the intended direction. The figure also shows that at the communication direction $\theta = -50°$, the proposed coherent phase-modulation based method achieves the best BER performance, while the single waveform sidelobe control based method has the worst BER performance. The proposed non-coherent based methods have identical performance at $\theta = -50°$. It can be observed from the figure that the BER for non-coherent broadcast method is not flat. This is because the radiation power within the sidelobe region is not constant (see Fig. 1). Finally, we observe from the figure that the sidelobe control based method with waveform diversity has slightly better performance than the non-coherent phase-modulation based methods. However, it requires the use of $K = 8$ orthogonal waveforms while the non-coherent methods require only two orthogonal waveforms.

Example 5: DOA Estimation Performance

The final example evaluates the DOA estimation performance of the radar operation. We use the setup parameters from Examples 1 and 2. We assume two interfering reflectors that are located in the far-field at angles $-52°$ and $-48°$, respectively. This means that the sources are located in the vicinity of the intended communication direction $\theta_c = -50°$. The target reflection coefficients are assumed to be constant during each radar pulse, but change from pulse to pulse and are drawn from a normal distribution. The number of radar receive array elements is chosen as $N = 10$. The number of pulses used is 100, i.e., 100 data snapshots are used at the radar receiver to build the data covariance matrix. The MUSIC algorithm is used to perform DOA

estimation for all methods tested. The two targets are assume to be resolved provided

$$\left|\hat{\theta}_i - \theta_i\right| \leq \frac{\left|\theta_2 - \theta_1\right|}{2}, \quad i = 1, 2, \tag{34}$$

is satisfied [46]. The root-mean square error (RMSE) and the probability of target resolution are averaged over 500 independent runs. Figs. 7 and 8 depict the RMSE versus SNR and the probability of target resolution versus SNR, respectively. It can be observed from the two figures that the three proposed phase-modulation based methods outperform the method of [19] and [21]. This is because, for the proposed methods, the SLL remains the same during the whole coherent processing interval. Therefore, any reflections from clutter or interference targets remain homogeneous during the entire coherent processing interval. On the other hand, the methods of [19] and [21] modulate the SLL towards the communication direction which results in nonhomogeneous clutter and/or interference at the radar receiver. As a result, the DOA estimation performance deteriorates which affects subsequent radar processing steps that depend on the estimated DOAs.

VI. Conclusion

We have developed a novel dual-function radar-communication system in which information embedding is achieved through phase modulation. A bank of transmit beamforming weight vectors is designed to provide the same power radiation pattern to satisfy in the radar function requirements, whereas the signal phase toward the intended communication directions is chosen from a predefined constellation so that communication information can be embedded. The communication receiver detects the phase of the received signal and uses it to decode the embedded binary sequence. The proposed technique allows information delivery to the intended communication receiver regardless of whether it is located in the main- or side-lobe regions. Three signaling strategies were developed for coherent communications, non-coherent communications, and non-coherent broadcasting, respectively. The performance of the proposed techniques was investigated in terms of the BER, and the superiority of the proposed method was clearly demonstrated.

References

[1] Griffiths, H., Blunt, S., Chen, L., Savy, L., "Challenge problems in spectrum engineering and waveform diversity," in *Proc. IEEE Radar Conf. (RadarCon 2013)*, Ottawa, ON, Canada, Apr.–May 2013, pp. 1–5.

[2] Deng, H., Himed, B., "Interference mitigation processing for spectrum-sharing between radar and wireless communications systems," *IEEE Transactions on Aerospace and Electronic Systems*, vol. 49, no. 3, pp. 1911–1919, July 2013.

[3] Bliss, D., "Cooperative radar and communications signaling: The estimation and information theory odd couple," in *Proc. IEEE Radar Conf. (RadarCon 2014)*, Cincinnati, OH, May 2014, pp. 50–55.

[4] Hayvaci, H., Tavli, B., "Spectrum sharing in radar and wireless communication systems: A review," in *Proc. Int. Conf. Electromagnetics in Advanced Applications (ICEAA 2014)*, pp. 810–813, Aug. 2014, pp. 810–813.

[5] Baylis, C., Fellows, M., Cohen, L., Marks, R., "Solving the spectrum crisis: Intelligent, reconfigurable microwave transmitter amplifiers for cognitive radar," *IEEE Microwave Magazine*, vol. 15, no. 5, pp. 94–107, July-Aug. 2014.

[6] Paisana, F., Marchetti, N., DaSilva, L., "Radar, TV and cellular bands: Which spectrum access techniques for which bands?," *IEEE Communications Surveys & Tutorials*, vol. 16, no. 3, pp. 1193–1220, Third Quarter 2014.

[7] Huang, K.-W., Bica, M., Mitra, U., Koivunen, V., "Radar waveform design in spectrum sharing environment: Coexistence and cognition," in *Proc. IEEE Radar Conference (RadarCon)*, Arlington, VA, May 2015, pp. 1698–1703.

[8] Griffiths, H., Cohen, L., Watts, S., Mokole, E., Baker, C., Wicks, M., Blunt, S., "Radar spectrum engineering and management: Technical and regulatory issues," *Proc. IEEE*, vol. 103, no. 1, pp. 85–102, Jan. 2015.

[9] Mealey, R., "A method for calculating error probabilities in a radar communication system," *IEEE Trans. Space Electronics and Telemetry*, vol. 9, no. 2, pp. 37–42, Jun. 1963.

[10] Jamil, M., Zepernick, H., Pettersson, M., "On integrated radar and communication systems using Oppermann sequences," in *Proc. IEEE Military Communications Conf. (MILCOM 2008)*, San Diego, CA, Nov. 2008, pp. 1–6.

[11] Blunt, S., Yatham, P., Stiles, J., "Intrapulse radar-embedded communications," *IEEE Trans. Aerospace and Electronic Systems*, vol. 46, no. 3, pp. 1185–1200, July 2010.

[12] Blunt, S., Yatham, P., Stiles, J., "Embedding information into radar emissions via waveform implementation," in *Proc. Int. Waveform Diversity & Design Conf.*, Niagara Falls, Canada, Aug. 2010, pp. 8–13.

[13] Blunt, S., Metcalf, J., Biggs, C., Perrins, E., "Performance characteristics and metrics for intra-pulse radar-embedded communications," *IEEE Journal on Selected Areas in Communications*, vol. 29, no. 10, pp. 2057–2066, Dec. 2011.

[14] Ciuonzo, D., De Maio, A., Foglia, G., Piezzo, M., "Intrapulse radar-embedded communications via multi-objective optimization," *IEEE Trans. Aerospace and Electronic Systems*, vol. 51, no. 4, pp. 2960–2974, Oct. 2015.

[15] Surender, S., Narayanan, R., Das, C., "Performance analysis of communications & radar coexistence in a covert UWB OSA system," in *Proc. IEEE Global Commun. Conf. (GLOBECOM 2010)*, Miami, FL, Dec. 2010, pp. 1–5.

[16] Guerci, J., *Cognitive Radar: The Knowledge-Aided Fully Adaptive Approach*. Artech House, 2010.

[17] Goldsmith, A. and Greenstein, L., *Principles of Cognitive Radio*. Cambridge University Press, 2012.

[18] Haykin, S., *Cognitive Dynamic Systems: Perception-Action Cycle, Radar and Radio*. Cambridge University Press, 2012.

[19] Euziere, J., Guinvarc'h, R., Lesturgie, M., Uguen, B., Gillard, R., "Dual function radar communication time-modulated array," in *Proc. Int. Radar Conf.*, Lille, France, Oct. 2014.

[20] Geng, Z., Deng, H., Himed, B., "Adaptive radar beamforming for interference mitigation in radar-wireless spectrum sharing," *IEEE Signal Processing Letters*, vol. 22, no. 4, pp. 484–488, Apr. 2015.

[21] Hassanien, A., Amin, M., Zhang, Y., Ahmad, F., "A dual function radar-communications system using sidelobe control and waveform diversity," in *Proc. 2015 IEEE Int. Radar Conf. (RadarCon 2015)*, Arlington, VA, May 2015.

[22] Hassanien, A., Amin, M., Zhang, Y., Ahmad, F., "Dual-function radar-communications: Information embedding using sidelobe control and waveform diversity," *IEEE Trans. Signal Processing*, In Press, 2016.

[23] Guerci, J., Guerci, R., Lackpour, A., Moskowitz, D., "Joint design and operation of shared spectrum access for radar and communications," in *Proc. 2015 IEEE Int. Radar Conf. (RadarCon 2015)*, Arlington, VA, May 2015.

[24] Hassanien, A., Amin, M., Zhang, Y., Ahmad, F., "Dual-Function Radar-Communications Using Phase-Rotational Invariance," in *Proc. European Signal Processing Conf. (EUSIPCO'2015)*, Nice, France, Aug.-Sept. 2015.

[25] Khawar, A., Abdelhadi, A., Clancy, C., "Target detection performance of spectrum sharing MIMO radars," *IEEE Sensors Journal*, vol. 15, no. 9, pp. 4928–4940, Sept. 2015.

[26] He, H., Stoica,P., Li, J., "Waveform design with stopband and correlation constraints for cognitive radar," in *Proc. 2nd Int. Workshop on Cognitive Information Processing*, Elba Island, Italy, June 2010, pp.344–349.

[27] Sit, Y., Sturm, C., Reichardt, L., Zwick, T., Wiesbeck, W., "The OFDM joint radar-communication system: An overview," in *Proc. Int. Conf. Advances in Satellite and Space Communications (SPACOMM 2011)*, 2011, pp. 69–74.

[28] Patton2012 Patton, L., Bryant, C., Himed, B., "Radar-centric design of waveforms with disjoint spectral support" in *Proc. IEEE Radar Conference (RadarCon)*, May 2012, pp. 1106–1110.

[29] Aubry, A., De Maio, A., Piezzo, M., Farina, A., "Radar waveform design in a spectrally crowded environment via nonconvex quadratic optimization," *IEEE Trans. Aerospace and Electronic Systems*, vol. 50, no. 2, pp. 1138–1152, Apr. 2014.

[30] Aubry, A., De Maio, A., Huang, Y., Piezzo, M., Farina, A., "A new radar waveform design algorithm with improved feasibility for spectral coexistence," *IEEE Trans. Aerospace and Electronic Systems*, vol. 51, no. 2, pp. 1029–1038, Apr. 2015.

[31] Li, J., Xu, L., Stoica, P., Forsythe, K., Bliss, D., "Range compression and waveform optimization for MIMO radar: A CramerRao bound based study," *IEEE Trans. Signal Processing*, vol. 56, no. 1, pp. 218–232, Jan. 2008.

[32] Li, J., Stoica, P., *MIMO Radar Signal Processing.* Wiley, 2009.

[33] Hassanien, A., Vorobyov, S., "Why the phased-MIMO radar outperforms the phased-array and MIMO radars?" in *Proc. 18th European Signal Processing Conf.*, Aalborg, Denmark, Aug. 2010, pp. 1234–1238.

[34] Ravan, M., Adve, R., Riddolls, R., "MIMO fast fully adaptive processing in over-the-horizon radar," in *Proc. 2015 IEEE Int. Radar Conf. (RadarCon 2011)*, Kansas City, MO, May. 2011, pp. 538–542.

[35] Hassanien, A., Vorobyov, S., "Transmit energy focusing for DOA estimation in MIMO radar with colocated antennas," *IEEE Trans. Signal Processing*, vol. 59, no. 6, pp. 2669–2682, June 2011.

[36] Zhang, Y., Amin, M., Himed, B., "Joint DOD/DOA estimation in MIMO radar exploiting time-frequency signal representations," *EURASIP Journal on Advances in Signal Processing*, vol. 2012, no. 1, July 2012.

[37] Khabbazibasmenj, A., Hassanien, A., Vorobyov, S., Morency, M., "Efficient transmit beamspace design for search-free based DOA estimation in MIMO radar," *IEEE Trans. Signal Process.*, vol. 62, no. 3, pp. 1490–1500, Mar. 2014.

[38] Hassanien, A., Amin, M., Zhang, Y., Ahmad, F., "Capon-based single snapshot DOA estimation in monostatic MIMO Radar," in *Proc. Symposium SPIE Sensing Technology + Applications*, Baltimore, MD, Apr. 2015.

[39] Hassanien, A., Amin, M., Zhang, Y., Ahmad, F., "High-resolution single-snapshot DOA estimation in MIMO radar with colocated antennas," in *Proc. 2015 IEEE Int. Radar Conf. (RadarCon 2015)*, Arlington, VA, May 2015.

[40] Boyd, S., Vandenberghe, L., *Convex Optimization.* Cambridge University Press, 2009.

[41] Hassanien, A., Vorobyov, S., Khabbazibasmenj, A., "Transmit radiation pattern invariance in MIMO radar with application to DOA estimation," IEEE Signal Processing Lett., vol. 22, no. 10, pp. 1609–1613, Oct. 2015.

[42] Khabbazibasmenj, A., Hassanien, A., Vorobyov, S., "How many beamforming vectors generate the same beampattern?" arXiv preprint, arXiv:1402.1682, 2014.

[43] Alabaster, C., *Pulse Doppler Radar: Principles, Technology, Applications.* SciTech Publishing, 2012.

[44] Levanon, N., "Mitigating range ambiguity in high PRF radar using inter-pulse binary coding," *IEEE Trans. Aerospace and Electronic Systems*, vol. 45, no. 2, pp. 687–697, Apr. 2009.

[45] Meikle, H., *Modern radar systems*. Artech House, 2008.

[46] Van Trees, H., *Optimum Array Processing*. *Wiley*, NY, 2002.
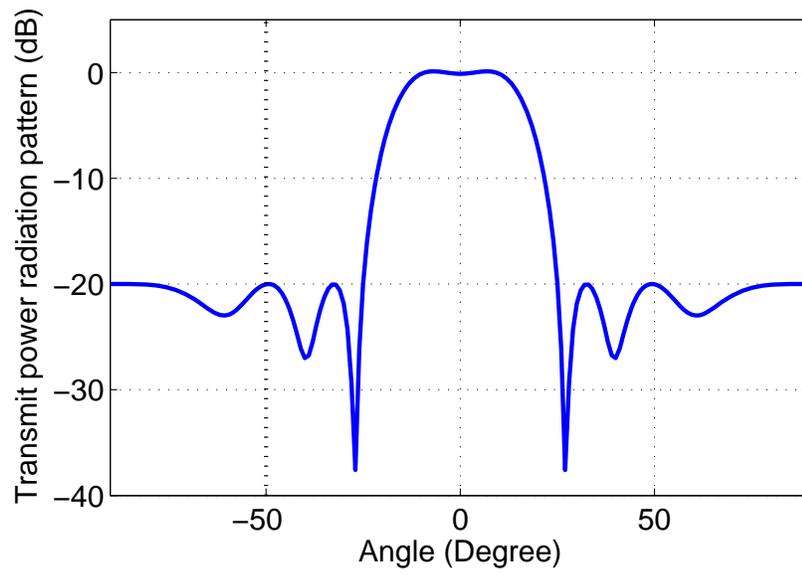
Fig. 1. Transmit power radiation pattern versus spatial angle; Example 1.
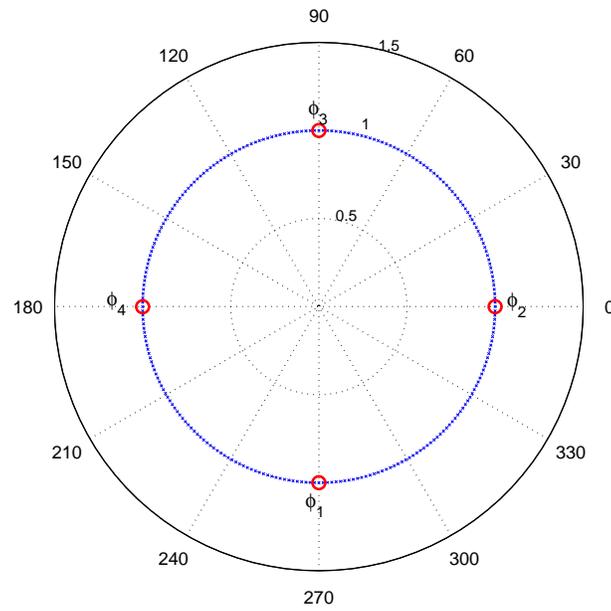
Fig. 2. Phase-rotation distribution versus spatial angle for a population of 512 pairs of transmit beamforming weight vectors; Example 1.
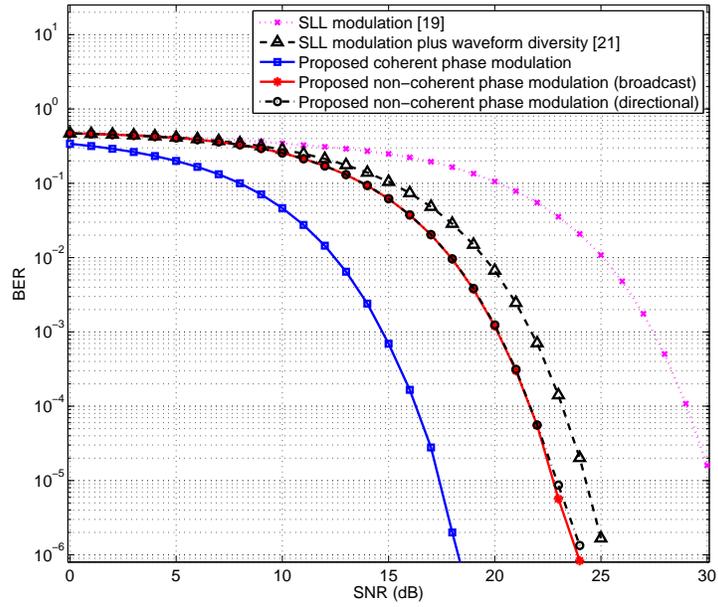
Fig. 3. BER versus SNR for $\theta_c = -50°$; Example 2.
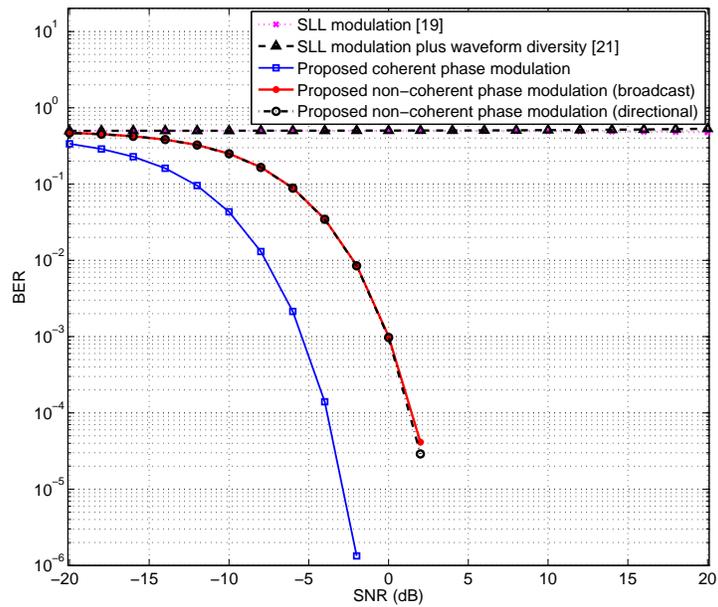
Fig. 4. BER versus SNR for $\theta_c = 7.5°$; Example 3.
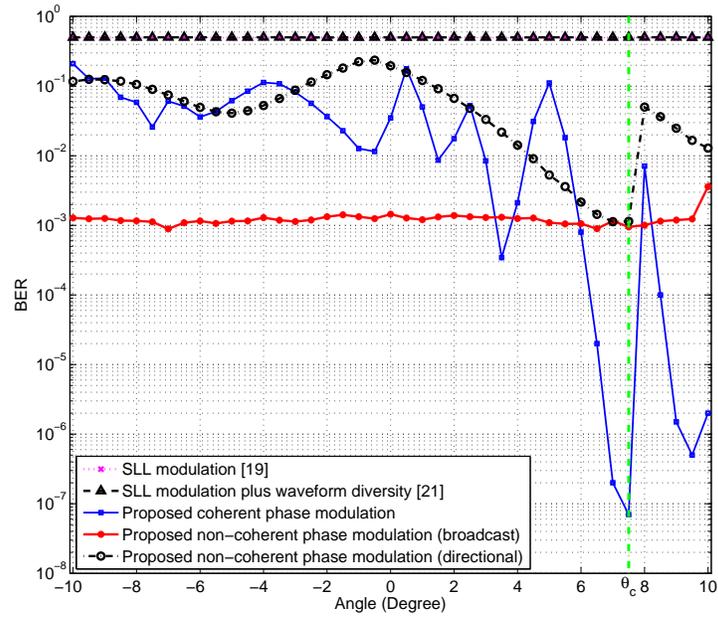
Fig. 5.   BER versus spatial angle (intended communication receiver located in main radar beam at $\theta = 7.5°$); Example 4.
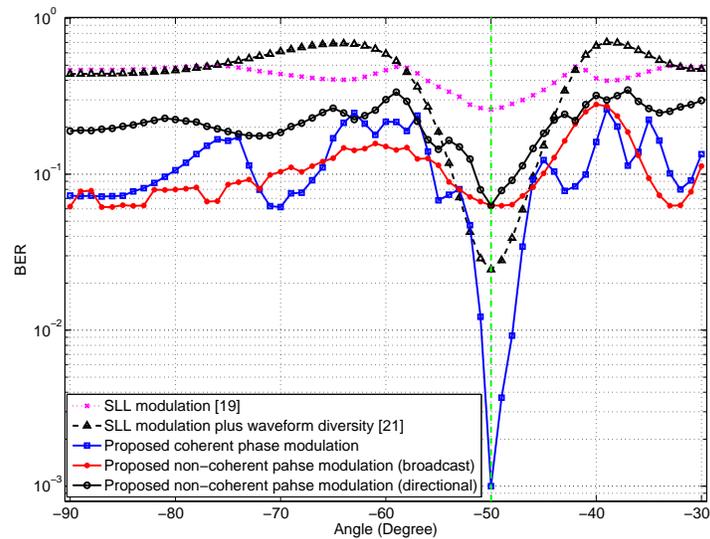

Fig. 6.   BER versus spatial angle (intended communication receiver located in sidelobe region at $\theta = -50°$); Example 4.
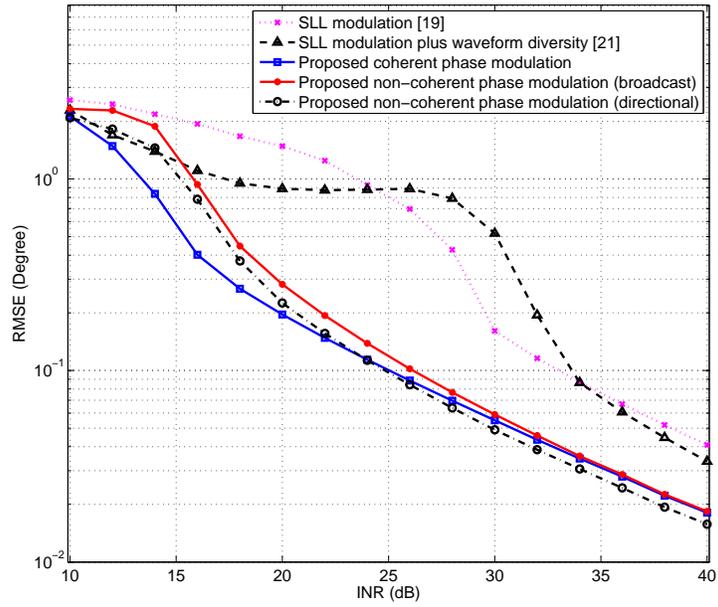
Fig. 7.   RMSE versus SNR; Example 5.
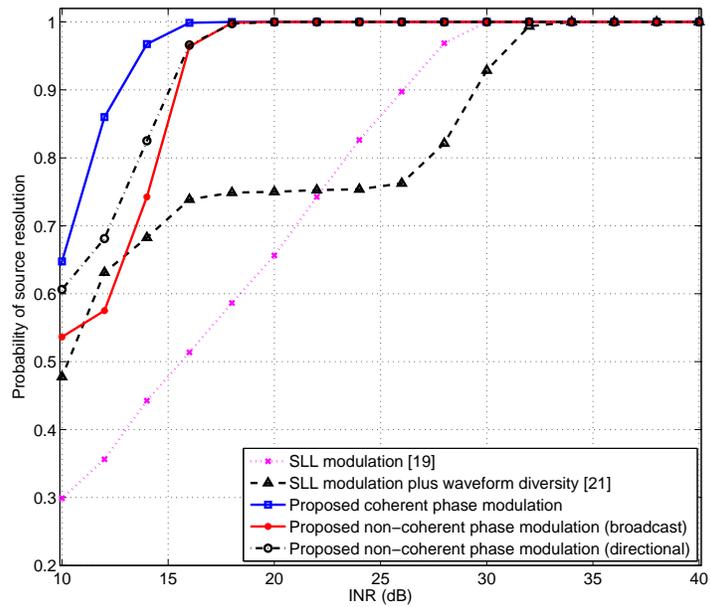
Fig. 8.   Probability of source resolution versus SNR; Example 5.